Water Disinfection by Pulsed Atmospheric Air Plasma Along Water Surface

Chao Zheng, Yuzhen Xu, Haomin Huang, Zhicheng Zhang, Zhen Liu, and Keping Yan
Key Laboratory of Biomass Chemical Engineering of Ministry of Education, Zhejiang University, Hangzhou 310007, China

Industrial Ecology and Environment Research Institute, Dept. of Chemical and Biological Engineering, Zhejiang University, Hangzhou 310007, China

Anna Zhu
Institute of Chemical Defense, Beijing 102205, China

DOI 10.1002/aic.13929
Published online October 15, 2012 in Wiley Online Library (wileyonlinelibrary.com).

An above water-pulsed nonthermal plasma technique for water disinfection is reported. Experiments are performed with a 2.5 L plasma reactor and Escherichia coli. When its initial number density is less than 10^6 cfu/mL, up to six orders reduction can be achieved within 0.5–2.5 min and at a plasma energy density of less than 2 J/mL. The disinfection performance is always effective by controlling water conductivity of below 1.5 mS/cm, which significantly affects plasma generation. Aqueous hydrogen peroxide, ozone, and nitric acid are continuously accumulated inside the reactor by the processing. Plasma generated UV radiation plays an important role in the cell inactivation. Inactivated cell morphology almost remains the same shape, their intracellular protein like green fluorescent protein, however, is destructed according to fluorescence observation. © 2012 American Institute of Chemical Engineers *AIChE J,* 59: 1458–1467, 2013
Keywords: water disinfection, nonthermal plasma, pulsed-power technology, E. coli

Introduction

Water disinfection is usually based on adding chemicals. Their by-products may lead to health side-effects.[1] Pulsed electrical field (PEF) and nonthermal plasma (NTP) techniques have been considered as friendly physical techniques because of their efficiency and safety.[2] PEF is realized by placing two electrodes inside water and applying a voltage pulse between the two electrodes to generate a peak electric field of around 20–90 kV/cm but without leading to electrical breakdown. However, NTP is generated by high voltage discharges inside water and/or above water surface. Ultraviolet radiation, shock waves, strong electromagnetic fields, and active species, such as OH radicals, hydrogen peroxide, and ozone are generated in both gaseous and aqueous phases.[3,4] Plasma-induced damages on DNA, protein, and biomacromolecule have been reported in order to understand the disinfection processes.[5–7]

Disinfection depends on a number of factors, such as plasma sources, plasma energy density, treatment time, containments, and temperature.[8] The group led by Mizuno reported that the cell destruction is very cost effective when using nonuniform electrode geometries and producing aqueous arc discharges. The energy consumption is about 21–42 J/mL to achieve six orders of yeast cell reduction with a rod-rod reactor.[9] The order reduction is defined as the logarithm ratio of the initial cell density over its survival value. Ching reported that when using a 3 L rod-rod reactor for treating *E. coli* suspended in 0.01 mol/L phosphate buffer saline, the order reduction is 2.1 under an energy density of around 100 J/mL and initial cell density of 4×10^7 cfu/mL.[10] Abou-Ghazala reported that using a wire-plate reactor the energy densities are 10 J/mL and 40 J/mL for three orders reduction of *E. coli* and *B. subtilis*, respectively.[11] Vaze reported that underwater spark discharge can lead to four orders reduction of 10^7 cfu/mL *E. coli* under the energy density of around 2 J/mL. For 4.5 orders reduction of 10^5 cfu/mL, it is about 0.8 J/mL.[12] For continuous processing, Fudamoto reported that with a wire-cylinder reactor the energy density rises 10 times higher than that for batch processing to achieve the same reduction level. The maximum inactivation rate is about 85% under the energy density of 35 J/mL.[13] For treating *Pseudomonas putida* in fresh water, Gupta found that the energy density is about 20 J/mL for six orders reduction with a wire-cylinder reactor, it rises, however, to 180 J/mL to get two orders reduction when wastewater conductivity becomes 1.2 mS/cm.[14] For treating tap water with a conductivity of 0.1 mS/cm and the initial cell density of 10^6 cfu/mL, Anpilov reported that with a multielectrode slipping surface discharge system, the energy densities for one order reduction of *E. coli* and coliphage are 0.3 J/mL and 0.15 J/mL, respectively.[15] Anpilov also found

Correspondence concerning this article should be addressed to K. Yan at kyan@zju.edu.cn.

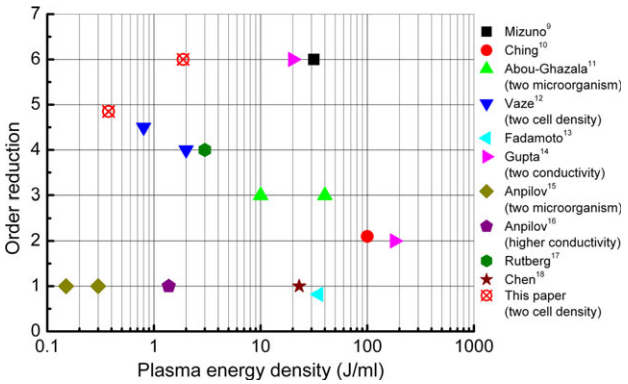

Figure 1. Over review of the relationship between the plasma energy density and the order reduction of microorganisms.[9–18]

[Color figure can be viewed in the online issue, which is available at wileyonlinelibrary.com.]

that for treating wastewater with conductivity of 0.9–1.4 mS/cm, the energy is about 1.25–1.5 J/mL to achieve one order reduction.[16] For the PEF technique, Wan recently reviewed its effectiveness for liquid food disinfection, the energy density is in the range of 30–7541 J/mL for achieving one to six orders of microbial reduction.[2] For the above water discharge systems, one electrode is usually placed inside water and the another electrode is placed above the water surface. Rutberg reported a needle-plate reactor with underwater needle electrode and plate electrode placed above the water surface, four orders reduction of *E. coli* of 10^6 cfu/mL was achieved at 3 J/mL.[17] Using a needle-plate reactor with overwater needle electrode, Chen reported that for treating *E. coli* of 10^5–10^6 cfu/mL, 23 J/mL plasma energy is required to get one order reduction.[18]

Reviewing over 20 years investigations on plasma-induced water disinfection, Figure 1 summarizes available reports in terms of the plasma energy density and the order reduction of those microorganisms. We can conclude that plasma source techniques, the initial cell density and water conductivity significantly affect the required energy density. It is also impossible to get an obvious relation between these plasma techniques and the disinfection efficiency. The required plasma energy consumption changes over 100 times for similar order reduction. Further detailed investigations on fundamental mechanisms of both plasma generation and disinfection effectiveness are required in order to get a deep insight on the technique.

This article presents our recent work on pulsed plasma induced water disinfection or cell inactivation with a homemade pulsed power source and an above water plasma reactor. All experiments are performed with *E. coli* in order to evaluate the processes. The final objective of this work is to develop a NTP process for drinking water disinfection.

Experimental Setup and System Specification

Figure 2 shows a schematic diagram of the pulsed plasma system. It consists of a plasma reactor, a resonant charging source, a high-voltage capacitor (C_H), a multigap spark switch, an inductor L together with a capacitor C and a resistor R formed LCR trigger.[19] The 39.2 nF capacitor C_H is charged from 10 to 30 kV. Figure 3 shows the reactor photo. Its inner diameter and volume are 150 mm and 2.5 L, respectively. An air distributor is placed at its bottom for air

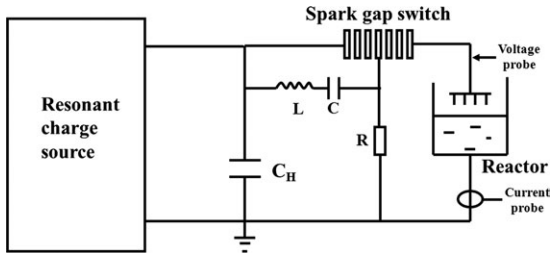

Figure 2. Schematic diagram of the experimental setup.

injection. Both air pressure and water flow rate can be individually adjusted. Water volume inside the reactor is usually 1.6 L. The whole reactor is grounded except the high voltage electrode which is separated by a Teflon insulator. The high voltage electrodes consist of four stainless steel needles, which are usually placed 1–10 mm above the water surface. Atmosphere air plasma is generated between the high voltage (HV) electrodes and the grounded reactor wall via the water surface. All experiments are performed with a pulse repetition rate of 2 pulses per second (pps). The plasma optical emission spectrum is obtained using a fiber optical spectrometer (Ocean optics HR2000+).

Two current probes as shown in Figure 4A are used to monitor current distribution. The plate current probe is placed 2 cm below the water surface. The obtained current is called underwater current. The difference between the total current and the underwater current is defined as the plasma current along the water surface. All electrical measurements are recorded with the Tektronix oscilloscope (DPO 7054, 500 MHz). In order to investigate effects of UV radiation on the *E. coli* disinfection, two quartz tubes placed near the bottom and below the water surface as shown in Figure 4B are used to collect samples without directly treated by active species, such as radicals, but only with UV radiation and/or pressure wave.

E. coli MV1184 (pGLO) and ATCC25922 are used for experiments. Their number density is obtained by means of heterotrophic plate count method. The *E. coli* ATCC25922 is used to evaluate the disinfection efficiency. It is firstly cultivated for 8–10 h at 37°C in a prepared Luria-Bertani (LB) medium, which consists of 10 g/L of peptone, 5 g/L of yeast extract, and 10 g/L of sodium chloride. Its number density rises to about 10^9–10^{10} cfu/mL. Then, the *E. coli* is harvested by centrifugation and suspended in deionized water. All the disinfection experiments are performed twice and each sample is tested on three plates. *E. coli* MV1184 (pGLO) is used to investigate plasma effectiveness on intracellular protein.

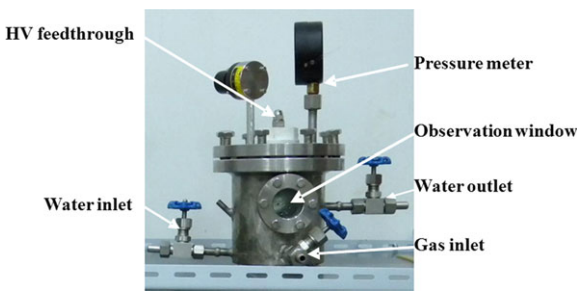

Figure 3. Reactor photo.

[Color figure can be viewed in the online issue, which is available at wileyonlinelibrary.com.]

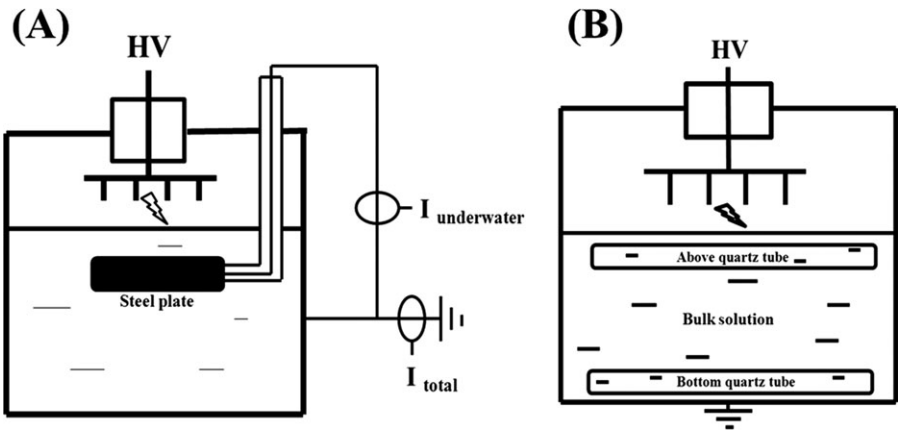

Figure 4. Systems layout: A. Underwater current probe, B. Two quartz tubes.

Green fluorescent protein (GFP) is produced inside the cells when 1.5 g/L L-Arabinose exists in the LB medium. The GFP fluorescence can be excited using 365 nm UV iradiation or fluorescent microscope (Nikon A1). For investigation on the plasma effects on the cell morphology, we use scanning electrical microscope (SEM; Philips XL30) for this work.

Results and Discussion

Effect of the plasma energy density on the disinfection

Figure 5 presents typical discharge voltage-current waveforms. Water conductivity is 3.5 μS/cm. The peak voltage, peak current and energy per pulse, voltage rise time, and pulse width are 18 kV, 2.5 kA, 10 J, 150 ns, and 10 μs, respectively. The peak voltage almost corresponds to zero current. It is a streamer-arc type pulsed plasma discharge.

Figure 6 shows typical cell survival curves under various applied voltages. The initial density of *E. coli* ATCC25922 is 6×10^6 cfu/mL. Cells are suspended in deionized water with a conductivity of 3.5 μS/cm. Disinfection efficiency rises by increasing the applied voltage from 12 kV to 18 kV. The energy per pulse for voltages of 12 kV, 15 kV, and 18 kV are 6 J, 8 J, and 10 J, respectively. Most cells are inactivated after 0.5 min processing. Disinfection becomes much less efficient after 1 min processing. When replotting the curves shown in Figure 6 in terms of the plasma energy density and the order reduction as shown in Figure 7, the disinfection efficiency is only dependent on the energy density but not on the voltage. The order reduction n can be approximated by

$$\frac{n}{n_\infty} = 1 - \exp\left(-\frac{\varepsilon}{\beta}\right)$$

where ε, n_∞, and β are the energy density, the maximum order number, and a coefficient, respectively.

Effect of the initial cell density on the disinfection

Figure 8 shows typical order reduction in terms of the plasma energy density and/or the treatment duration. Experiments are performed in deionized water and the applied voltage of 18 kV. Almost all *E. coli* ATCC25922 can be inactivated in 0.5 min or under 0.375 J/mL when the initial density is below 7.0×10^4 cfu/mL. For an initial value of 1.0×10^6 cfu/mL, it rises to 2.5 min. For 10^6–10^7 cfu/mL, the disinfection process becomes much less efficient after 1 min processing. There are 10–10^3 cfu/mL remained even after 2.5 min processing. For an initial density of 10^8–10^9 cfu/mL, only three orders reduction can be achieved after 2.5 min. With regard to the total inactivated cells, however, the

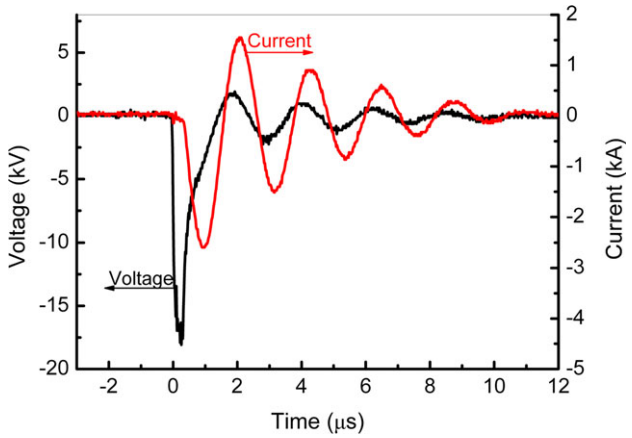

Figure 5. Typical voltage and current waveforms under water conductivity of 3.5 μS/cm.

[Color figure can be viewed in the online issue, which is available at wileyonlinelibrary.com.]

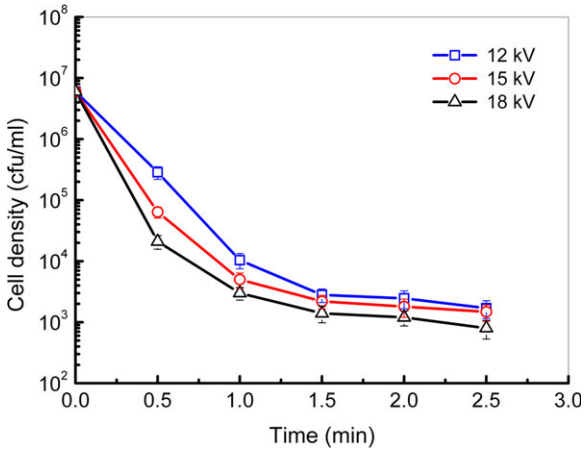

Figure 6. Typical cell survival curves under water conductivity of 3.5 μS/cm and initial cell density of 6×10^6 cfu/mL.

[Color figure can be viewed in the online issue, which is available at wileyonlinelibrary.com.]

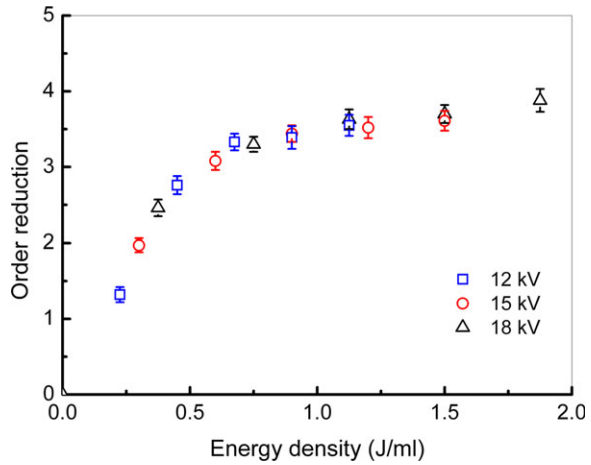

Figure 7. Orders reduction in terms of the plasma energy density under the applied voltage from 12 to 18 kV , water conductivity of 3.5 μS/cm and cell initial density of 6 × 10^6 cfu/mL.

[Color figure can be viewed in the online issue, which is available at wileyonlinelibrary.com.]

higher the initial density, the more the inactivated cells. For an initial value of 8.0 × 10^8 cfu/mL, the total inactivated *E. coli* cell number at three order reduction is nearly 1.28 × 10^{12} after 2.5 min treatments. For an initial value of 10^6 cfu/mL and six order reduction, it is only about 1.6 × 10^9 in total.

With regard to interactions between plasma and cells, it has been anticipated that both dead and live cells could react with plasma. As a result, there is a so-called "shield effect" when the initial density becomes high,[10] which results in the maximum reduction number as shown in Figure 9 in terms of the initial density, where the plasma energy density is less than 2 J/mL. For the initial number density of below 10^6 cfu/mL, the maximum value n_∞ is proportional to the initial value. It drops when the initial value becomes larger. In order to demonstrate this "shield effect," comparison experiments are performed again by adding autoclaved cells into the reactor as shown in Figure 10. When the live cells density is 1.5 × 10^5 cfu/mL, 2.5 orders reduction can be achieved after 0.5 min processing and all the cells are inactivated after 1 min. If adding 3.0 × 10^6 cfu/mL or 5.0 × 10^7 cfu/mL of autoclaved cells to the reactor, the order reduction in 0.5 min drops to 2.3 and 1.8, respectively. There are still live cells after 1 min processing. The autoclaved cells clearly show a "shield effect" for processing the live cells. We can also conclude that there is no significant shield effect for the initial density of below 10^6 cfu/mL. The plasma energy consumption is no larger than 1.875 J/mL (or 0.5 kWh/m^3) for up to six orders reduction.

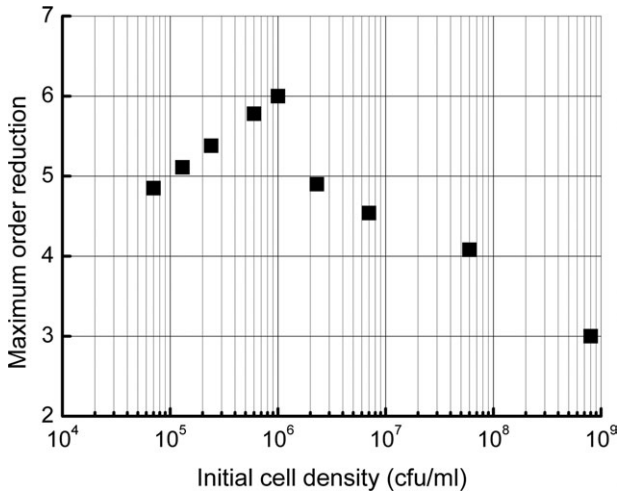

Figure 9. The maximum value of the order reduction in terms of the initial cell number density when the energy density is less than 2 J/mL.

Effect of water conductivity on the disinfection

Figure 11 shows corresponded plasma photos obtained with a digital camera and a narrowband optical filter under various conductivities, which are adjusted by adding potassium chloride into water. Plasma is usually generated from the electrode tip to the reactor wall via the water surface.

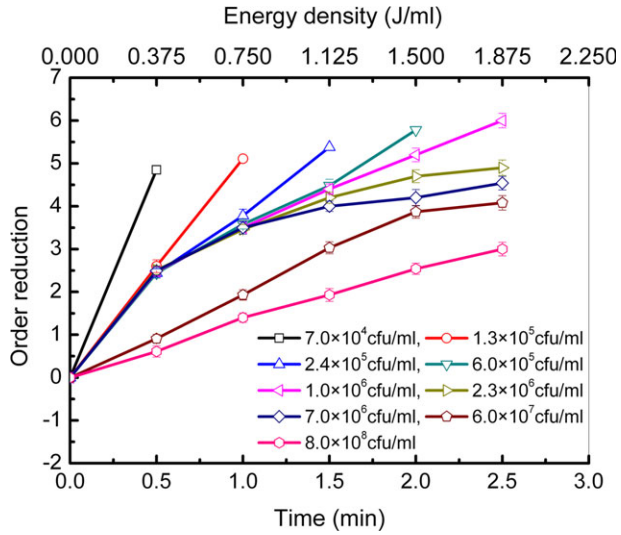

Figure 8. Effect of the initial cell density on disinfection efficiency under 18 kV and 3.5 μS/cm.

[Color figure can be viewed in the online issue, which is available at wileyonlinelibrary.com.]

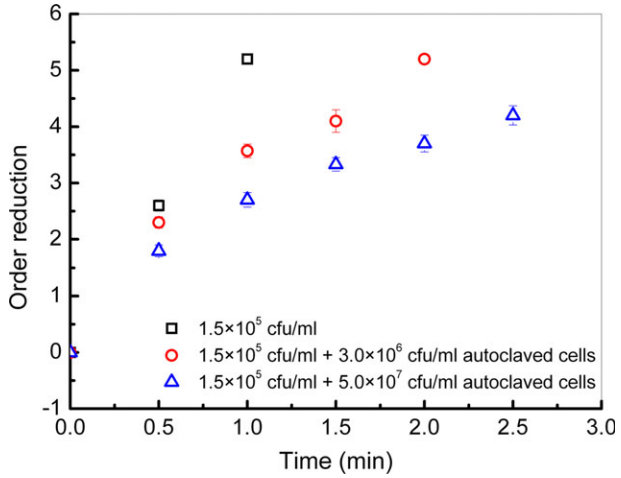

Figure 10. Effect of autoclaved *E. coli* cells on plasma disinfection.

[Color figure can be viewed in the online issue, which is available at wileyonlinelibrary.com.]

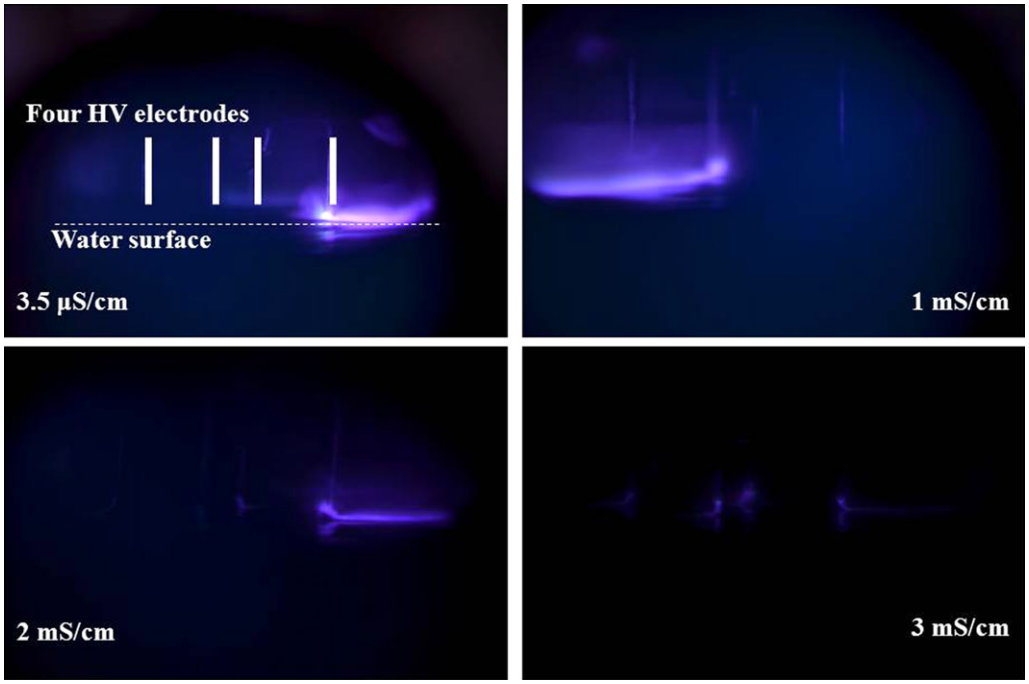

Figure 11. Stationary discharge photos under four water conductivities.

[Color figure can be viewed in the online issue, which is available at wileyonlinelibrary.com.]

High intensity plasma can only be generated when the conductivity is less than 2.0 mS/cm.

Figure 12 shows typical effects of the water conductivity on plasma current and voltage waveforms. The conductivity is in the range from 1.5 mS/cm to 5.0 mS/cm. With increasing the water conductivity, the peak voltage drops but the voltage width increases. At the same time, the peak current drops from 2.5 kA to 1.2 kA when it rises from 1.5 mS/cm to 5.0 mS/cm. The discharge energy, however, rises from 10 J/pulse to 13.6 J/pulse. The corresponded underwater current waveforms are shown in Figure 13. For a larger conductivity, such as 5 mS/cm, the underwater current shows a simple current pulse, corresponding to the first peak in Figure 12B. For a small conductivity, such as 1.5 mS/cm, its first peak value becomes much smaller but with a larger second peak and long oscillation. With regard to the system, we anticipate that the first peak current is simply due to electrical conduction and the later stage oscillation is due to the surface plasma dissipation. At the same time, we observed that after 2.5 min processing, the water temperature is increased by 0.1 and 0.5°C for the conductivities of 1.5 and 5.0 mS/cm, respectively. The higher the water conductivity, the more energy dissipated into water for heating. However, a detailed model is not available for analyzing current injection processes.

Figure 14 shows typical disinfection results in terms of the treatment duration and the order reduction under various water conductivities. All experiments are performed under an initial *E. coli* ATCC25922 density of 5×10^6 cfu/mL. When it is below 1.5 mS/cm, no significant effects on disinfection are observed and more than three orders reduction can be achieved after 1 min processing. For a value in between 2.0–3.5 mS/cm, the efficiency significantly drops and the required treatment duration becomes 2.5 min longer for the same reduction. If it becomes larger than 4.0 mS/cm, the process is no more effective for the present setup.

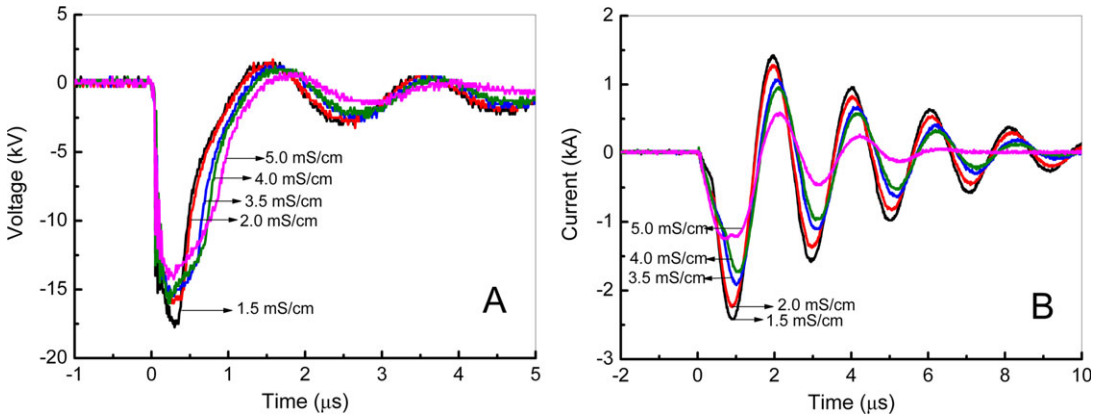

Figure 12. Voltage (A) and total current (B) waveforms under various conductivities.

[Color figure can be viewed in the online issue, which is available at wileyonlinelibrary.com.]

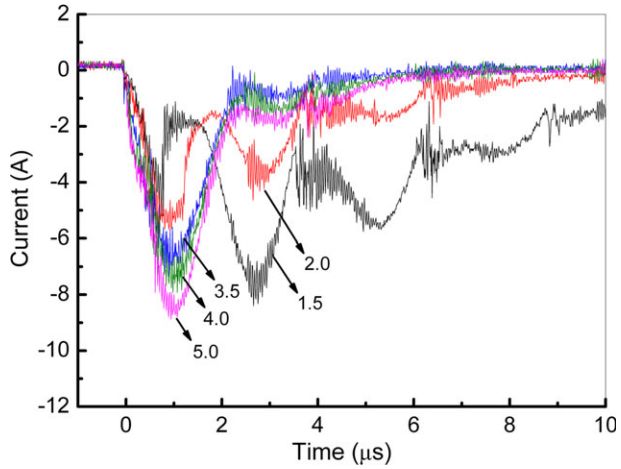

Figure 13. Underwater current waveforms under water conductivity of 1.5–5.0 mS/cm.

[Color figure can be viewed in the online issue, which is available at wileyonlinelibrary.com.]

Considering plasma photos in Figure 11 and disinfection in Figure 14, we conclude that when the conductivity becomes higher than 3 mS/cm, it is almost impossible to generate intensive surface plasma and/or to achieve high inactivation efficiency.

UV emission spectrum

UV emission spectrum of the pulsed atmospheric air plasma is obtained with a quartz window and an optical fiber spectrometer. Figure 15 shows the results under different water conductivities, which is in agreement with Figure 11. As conductivity rises, the light intensity drops significantly. When conductivity is below 1.5 mS/cm, intense UV emission is generated. If conductivity is over 5.0 mS/cm, light intensity becomes very weak. Intense germicidal UVC radiation of 230–300 nm is generated during discharge that indicates the important effect of UV radiation on disinfection. With regarding to radicals generated according to the emission spectrum, the contribution is mainly due to the NO_γ (230–290 nm), NO_β (270–380 nm), and hydroxyl radical of 309 nm bands.

Aqueous H_2O_2 and O_3 generation

As an indicator of the plasma reactivity, both aqueous hydrogen peroxide and ozone are detected by means of the iodide and indigo methods.[20] Figure 16 shows examples of hydrogen peroxide and ozone production in terms of the processing duration under 3.5 μS/cm. After 2.5 min processing, their concentrations reach 25 μmol/L and 1.5 μmol/L, respectively. The generated H_2O_2 is almost 15 times higher than O_3, which is very much different from traditional advanced oxidation technologies. Locke reviewed the hydrogen peroxide formation in various plasma processes. Most of the reported energy yield for hydrogen peroxide production is within 0.01–2.0 g/kWh.[21] It is 1.63 g/kWh for present system. For ozone, it is about 0.14 g/kWh. If *E. coli* cells are treated by the same amount of 25 μmol/L hydrogen peroxide and/or 1.5 μmol/L ozone without plasma, no significant inactivation is observed in 2.5 min. Experiments are also performed with using 10 mmol/L hydrogen peroxide but without plasma generation. The efficiency is less than 90% for 10 min processing of 10^6 cfu/mL *E. coli*, which is much lower in comparison with plasma processing.

Variation of aqueous pH value and conductivity

With regard to the pH value and the water conductivity during the 2.5 min discharge, as shown in Figure 17, the conductivity rises gradually from 3.5 μS/cm to 16 μS/cm while pH value drops from 7.0 to 4.8.

Aqueous nitric acid generation and UV absorption spectrum

As shown in Figure 18, the aqueous absorption for 200–240 nm rises with increasing the discharge period. In comparison with the spectrum of the standard nitric acid (25 μmol/L), they are very similar with a peak absorption around 210 nm. This is also in agreement with the UV emission spectrum in Figure 15, where reactive nitrogen radicals are generated. The derived nitric acid concentration after 2.5 min processing is 18 μmol/L, which is responsible for pH and conductivity variation. With regarding to their effects on the disinfection, we think that the acidity may not play a significant role for this work because of its small change from 6.6 to 6.3 when major inactivation is already realized in 0.5–1.0 min. If the pH drops to 2–3 as observed by Tang and Oehmigen,[22,23] acidity may play an important role for the cell inactivation.

Effects of water conductivity on aqueous H_2O_2 and nitric acid generation

Both Figures 11 and 15 show that the water conductivity significantly affects the discharge. Figure 19 shows the production of aqueous hydrogen peroxide and nitric acid after 2.5 min processing under different conductivities. Hydrogen peroxide and nitric acid are 25 μmol/L and 18 μmol/L when conductivity is 3.5 μS/cm. The concentration decreases as conductivity rises. For fresh water of around 200 μS/cm, it drops to 23.6 μmol/L and 14.1 μmol/L, respectively. When conductivity is 5.0 mS/cm, the values are only 14.3 μmol/L and 4.3 μmol/L, respectively.

Effect of plasma generated UV on the disinfection

In order to demonstrate UV effects on the disinfection, we conducted two types of experiments. One is by adding uridine to absorb UV and another one is using two quartz tubes placed 2 mm below water surface and on the reactor bottom

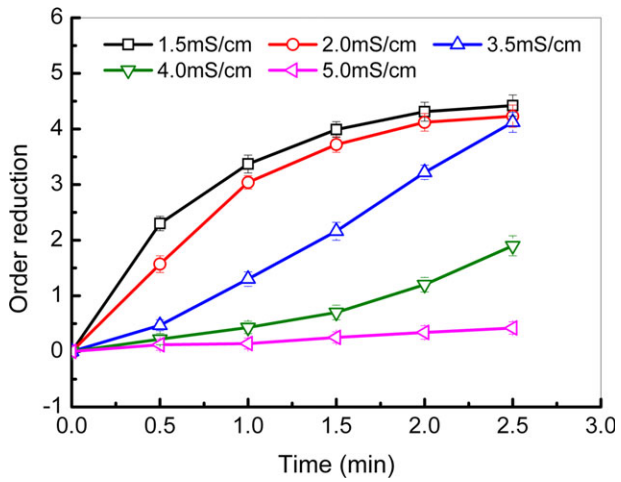

Figure 14. Effects of water conductivity on disinfection with initial cell density of 5×10^6 cfu/mL.

[Color figure can be viewed in the online issue, which is available at wileyonlinelibrary.com.]

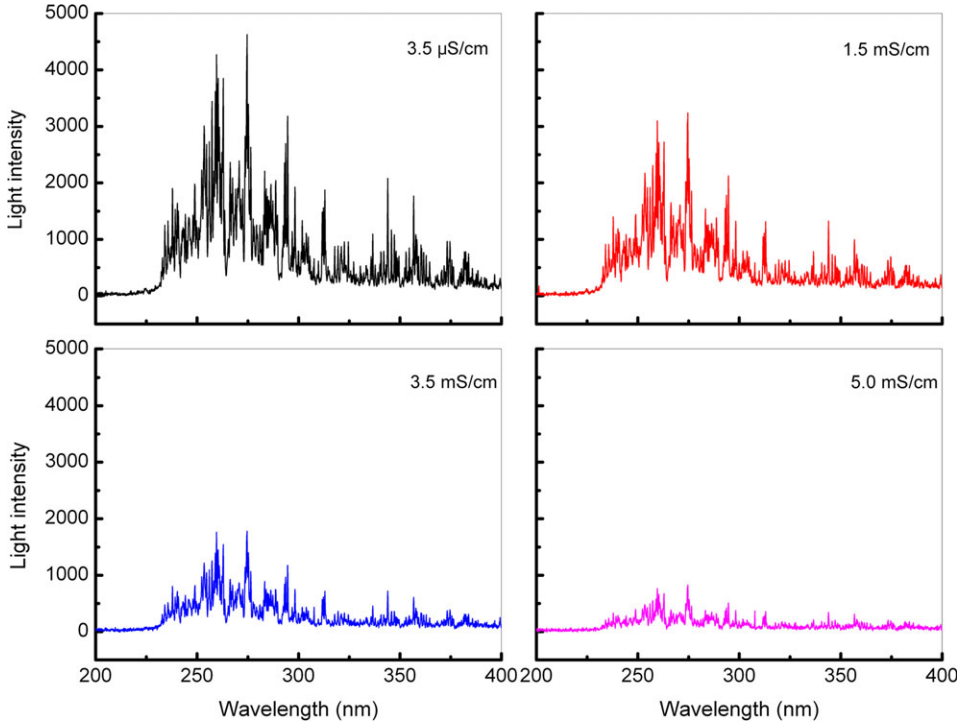

Figure 15. Variation of UV emission spectrum under different water conductivities.

[Color figure can be viewed in the online issue, which is available at wileyonlinelibrary.com.]

as shown in Figure 4B to collect individual smaples. Uridine is a very effective UV absorbent and has a similar UV absorption spectrum as DNA. The influences of uridine on the inactivation can indirectly reflect the UV effects on the inactivation. As an example, in comparsion without adding any uridine (blank), Figure 20 shows the effect of uridine when initial *E. coli* ATCC25922 density is 4.8×10^6 cfu/mL and water conductivity is 3.5 μS/cm. The disinfection is strongly inhibited as uridine concentration rises. If uridine concentration is higher than 1 mmol/L, the disinfection is no more effective for the present setup due to its UV absorption.

For the second type experiments, the initial *E. coli* ATCC25922 densities of inside and outside the tubes are 7×10^6 cfu/mL. Three series of samples from bulk solution and two quartz tubes are investigated. The orders reduction are shown in Figure 21. It is found that the orders reduction inside the tubes have similar trends with bulk solution. The disinfection efficiency in the above tube is a little higher than that in the bulk solution. And it is smaller for the bottom tube due to its distance to the surface discharge. More than four orders reduction of *E. coli* can be achieved after 2.5 min treatment in both quartz tubes. The cells inside the tubes are supposed to be mainly disinfected by UV radiation, which is in agreement with the observations by adding uridine as shown in Figure 20.

Cell morphology

In comparison with initial cell morphology, Figure 22 shows scanning electric microscope photos of *E. coli*

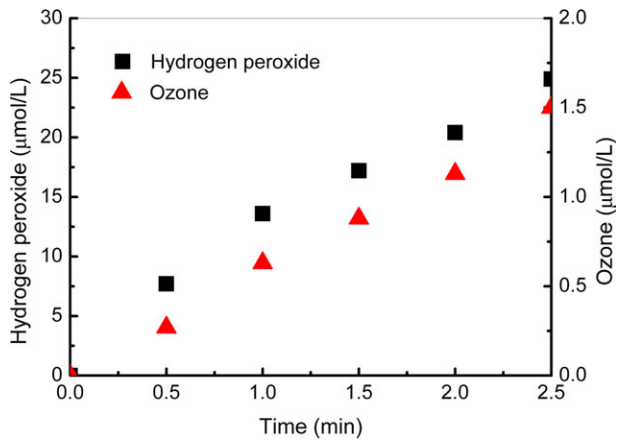

Figure 16. Production of aqueous hydrogen peroxide and ozone under 3.5 μS/cm.

[Color figure can be viewed in the online issue, which is available at wileyonlinelibrary.com.]

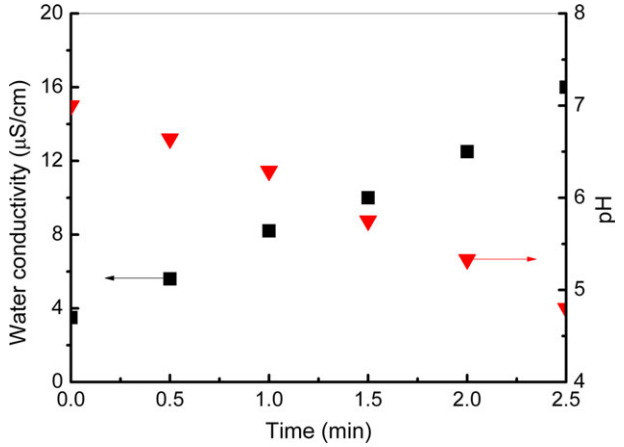

Figure 17. Variation of water conductivity and pH during plasma treatment under 3.5 μS/cm.

[Color figure can be viewed in the online issue, which is available at wileyonlinelibrary.com.]

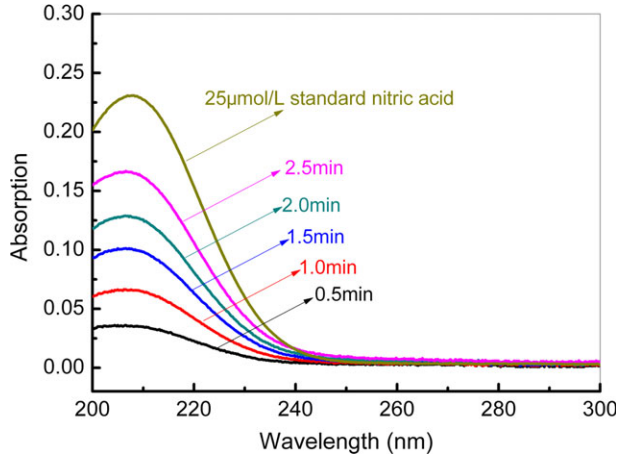

Figure 18. Variation of UV absorption spectrum during plasma treatment under 3.5 μS/cm.

[Color figure can be viewed in the online issue, which is available at wileyonlinelibrary.com.]

ATCC25922 after plasma processing. Its initial density is 2.8 $\times$ 10^7 cfu/mL. The cell survival curve is similar to Figure 8. Its order reduction are 1.1, 2.1, and 3.97 after 0.5, 1.0, and 2.5 min plasma treatment, respectively. More than 99.9% of the cells are inactivated. SEM photos show that almost all the cells are integral after the plasma inactivation, which are different from previous reports of cell disruption.[24–26]

Fluorescence variation and intracellular protein destruction

When using 365 nm UV irradiation, *E. coli* MV1184 cells emit intense green fluorescence which can be recorded directly by an digital camera. As examples, the fluorescence variation after plasma treatments is shown in Figure 23 when initial cell density is 1.8 $\times$ 10^7 cfu/mL. Its cell survival curve is similar to that in Figure 9. Most of the cells are inactivated in the first 0.5 and 1 min. The observation of fluorescence variation is in agreement with its survial curve. Light intensity of fluorescence also decreases significantly in the first 0.5 and 1 min.

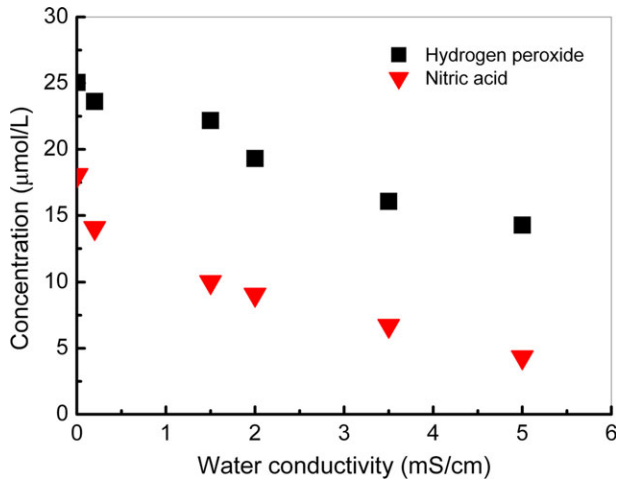

Figure 19. Production of aqueous hydrogen peroxide and nitric acid after 2.5 min treatment under different conductivities.

[Color figure can be viewed in the online issue, which is available at wileyonlinelibrary.com.]

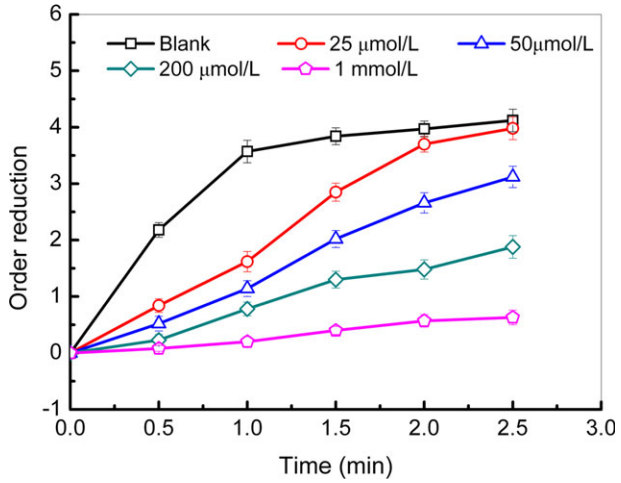

Figure 20. Effects of uridine on water disinfection when initial cell density is 4.8 $\times$ 10^6 cfu/mL.

[Color figure can be viewed in the online issue, which is available at wileyonlinelibrary.com.]

The same samples as in Figure 23 are also detected using fluorescent microscope. Before plasma treatment, *E. coli* cells are with bright green fluorescence under microscope as shown in Figure 24A. The fluorescence inside each cell in Figure 24B becomes weak after 0.5 min plasma treatment. Most of the intracellular green fluorescence disappears after 1 min. When it is treated for more time, no more fluorescence can be detected with the present microscope. This is consistent with the results in Figure 23 and its survival curve. According to results in Figures 23 and 24, the intracellular GFP is supposed to be rapidly destructed during plasma disinfection as its fluorescence disappears. As the GFP inside the *E. coli* cells cannot be rapidly destructed by low concentration of hydrogen peroxide, ozone, nitric acid, or UV radiation alone, we anticipate that it is destructed by reactive radicals and/or synergetic UV radiation during the transitory discharge.

Conclusions

Based on present experimental studies on the *E. coli* disinfection, we can give the following remarks:

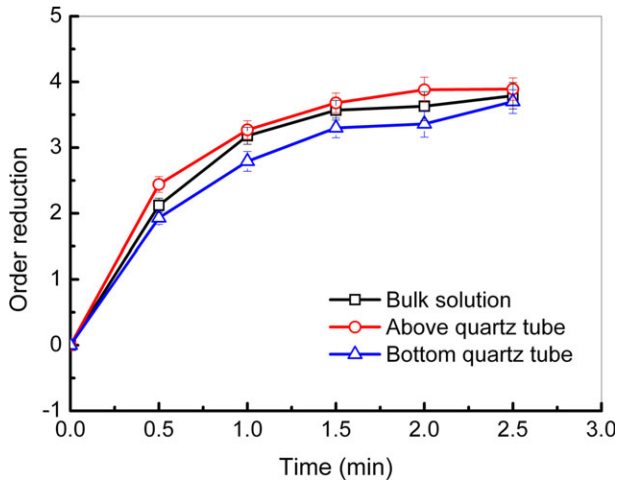

Figure 21. Water disinfection by UV radiation of plasma with initial cell density of 7 $\times$ 10^6 cfu/mL.

[Color figure can be viewed in the online issue, which is available at wileyonlinelibrary.com.]

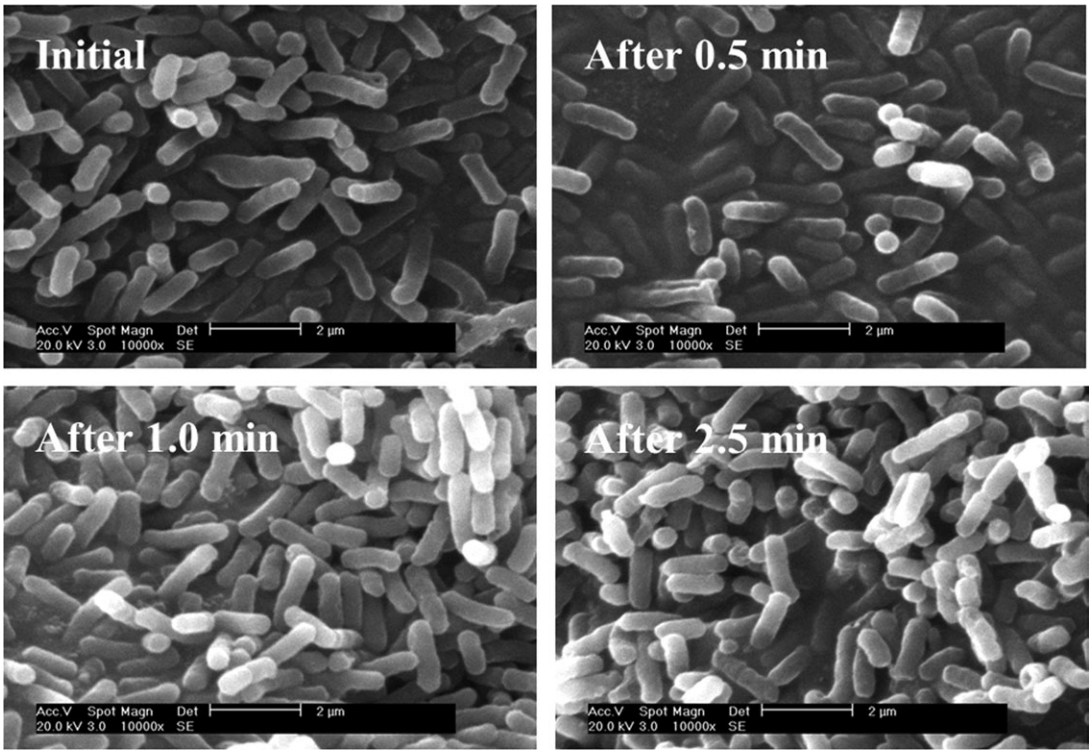

Figure 22. SEM photos after plasma treatments with initial cell density of 2.8×10^7 cfu/mL.

1. Water conductivity can significantly influence the generation of pulsed plasma, including the UV emission spectrum and reactive species. The disinfection is always effective when the water conductivity is smaller than 1.5 mS/cm. The energy consumption is around 0.3–1.9 J/mL for up to six order reduction.

2. The order reduction drops due to the shield effects when the initial density is higher than 10^6 cfu/mL but the

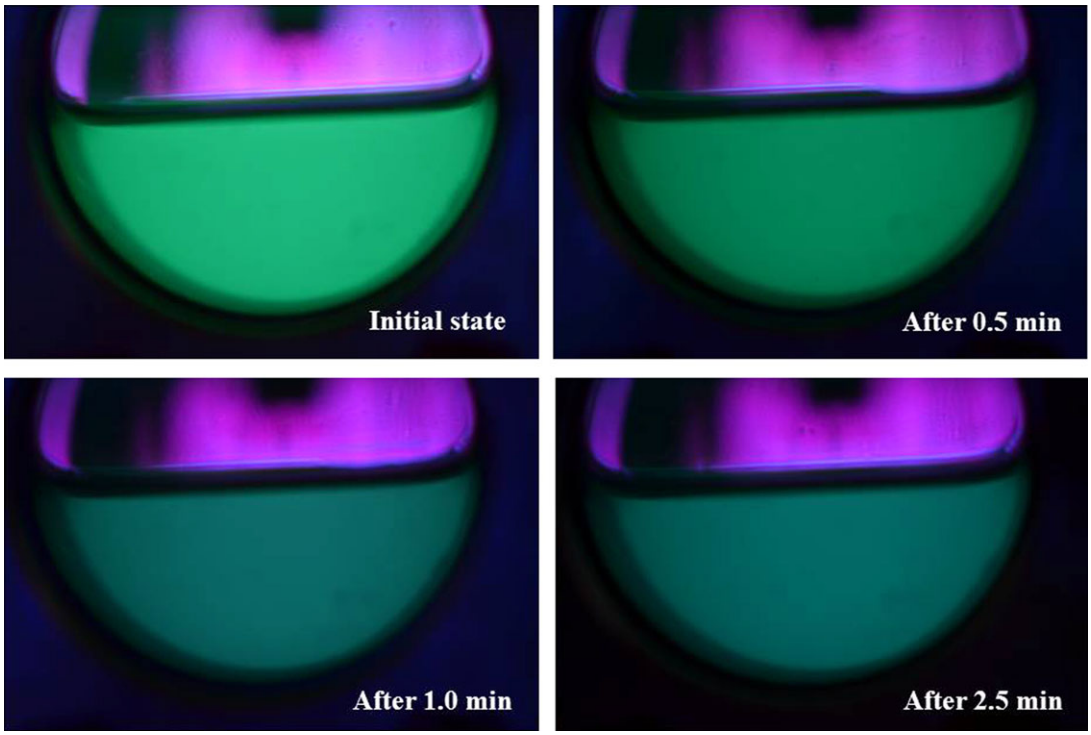

Figure 23. Fluorescence variation after plasma treatment when initial *E. coli* MV1184 density is 1.8×10^7 cfu/mL.

[Color figure can be viewed in the online issue, which is available at wileyonlinelibrary.com.]

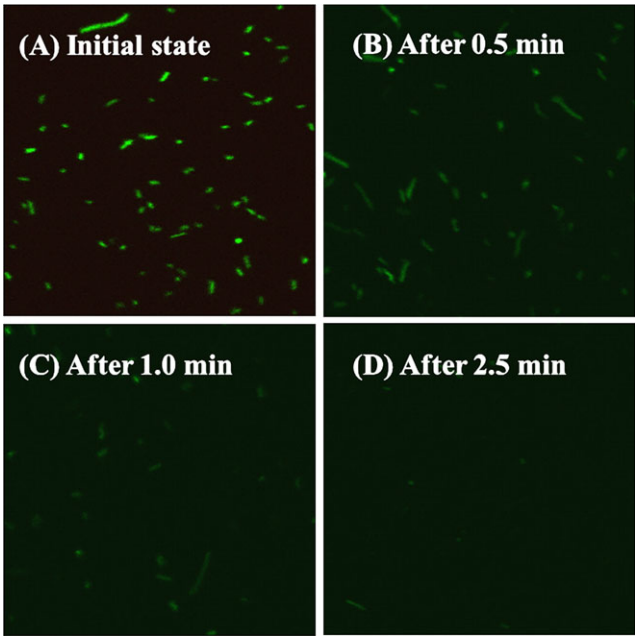

Figure 24. Fluorescent microscope photos of *E. coli* MV1184 after plasma treatment.

[Color figure can be viewed in the online issue, which is available at wileyonlinelibrary.com.]

total inactivated cell number rises with increasing the initial number concentration.

3. Plasma generated germicidal UV radiation plays an important role in disinfection. UV absorber such as uridine can greatly inhibit the process due to its UV absorption.

4. Plasma inactivated cells have the same morphology as live cells. Its intracellular protein like GFP, however, is rapidly destructed after plasma inactivation.

Acknowledgments

The authors would like to thank Prof. Akira Mizuno and Dr. Hachiro Yasuda of Toyohashi University of Technology, Japan, for valuable discussions.

Literature Cited

1. Hebert A, Forestier D, Lenes D, Benanou D, Jacob S, Arfi C, Lambolez L, Levi Y. Innovative method for prioritizing emerging disinfection by-products (DBPs) in drinking water on the basis of their potential impact on public health. *Water Res*. 2010;44:3147–3165.
2. Wan J, Coventry J, Swiergon P, Sanguansri P, Versteeg C. Advances in innovative processing technologies for microbial inactivation and enhancement of food safety-pulsed electric field and low-temperature plasma. *Trends Food Sci Technol*. 2009;20:414–424.
3. Sato M, Ohgiyama T, Clements JS. Formation of chemical species and their effects on microorganisms using a pulsed high-voltage discharge in water. *IEEE Trans Ind Appl*. 1996;32:106–112.
4. Xin Q, Zhang X, Lei L. Inactivation of bacteria in oil field injection water by non-thermal plasma treatment. *Plasma Chem Plasma Process*. 2008;28:689–700.
5. Yasuda H, Hashimoto M, Rahman MM, Takashima K, Mizuno A. States of biological components in bacteria and bacteriophages during inactivation by atmospheric dielectric barrier discharges. *Plasma Process Polym*. 2008;5:615–621.
6. Yasuda H, Miura T, Kurita H, Takashima K, Mizuno A. Biological evaluation of DNA damage in bacteriophages inactivated by atmospheric pressure cold plasma. *Plasma Process Polym*. 2010;7:301–308.
7. Perni S, Shama G, Hobman JL, Lund PA, Kershaw CJ, Hidalgo-Arroyo GA, Penn CW, Deng XT, Walsh JL, Kong MG. Probing bactericidal mechanisms induced by cold atmospheric plasmas with Escherichia coli mutants. *Appl Phys Lett*. 2007;90:073902.
8. Locke BR, Sato M, Sunka P, Hoffmann MR, Chang JS. Electrohydraulic discharge and non-thermal plasma for water treatment. *Ind Eng Chem Res*. 2006;45:882–905.
9. Mizuno A, Hori Y. Destruction of living cells by pulsed high-voltage application. *IEEE Trans Ind Appl*. 1988;24:387–394.
10. Ching WK, Colussi AJ, Sun HJ, Nealson KH, Hoffmann MR. Escherichia coli disinfection by electrohydraulic discharges. *Environ Sci Technol*. 2001;35:4139–4144.
11. Abou-Ghazala A, Katsuki S, Schoenbach KH, Dobbs FC, Moreira KR. Bacterial decontamination of water by means of pulsed-corona discharges. *IEEE Trans Plasma Sci*. 2002;30:1449–1453.
12. Vaze ND, Arjunan KP, Gallagher MJ, Vasilets VN, Gutsol A, Fridman A, Anandan S. *Air and water sterilization using non-thermal plasma*. In: *Proceedings of 16th IEEE International Pulsed Power Conference*, Albuquerque, USA, 2007:1231–1235.
13. Fudamoto T, Namihira T, Katsuki S, Akiyama H, Imakubo T, Majima T. Sterilization of E. coli by underwater pulsed streamer discharge in a continuous flow system. *Electr Eng Jpn*. 2008;164:669–674.
14. Gupta SB, Bluhm H. The potential of pulsed underwater streamer discharges as a disinfection technique. *IEEE Trans Plasma Sci*. 2008;36:1621–1632.
15. Anpilov AM, Barkhudarov EM, Christofi N, Kop'ev VA, Kossyi IA, Taktakishvili MI, Zadiraka Y. Pulsed high voltage electric discharge disinfection of microbially contaminated liquids. *Lett Appl Microbiol*. 2002;35:90–94.
16. Anpilov AM, Barkhudarov EM, Christofi N, Kop'ev VA, Kossyi A, Taktakishvili MI, Zadiraka YV. The effectiveness of a multi-spark electric discharge system in the destruction of microorganisms in domestic and industrial wastewater. *J Water Health*. 2004;2:267–277.
17. Rutberg PG, Kolikov VA, Kurochkin VE, Panina LK, Rutberg AP. Electric discharge and the prolonged microbial resistance of water. *IEEE Trans Plasma Sci*. 2007;35:1111–1118.
18. Chen CW, Lee HM, Chang MB. Inactivation of aquatic microorganisms by low-frequency ac discharge. *IEEE Trans Plasma Sci*. 2008;36:215–219.
19. Yan K, Heesch EJM van, Pemen AJM, Huijbrechts PAHJ, Laan PCT van. A 10 kW high-voltage pulse generator for corona plasma generation. *Rev Sci Instrum*. 2001;72:2443–2447.
20. Gupta SB. Investigation of a physical disinfection process based on pulsed underwater corona discharge. PhD Thesis, Karlsruhe Institute of Technology, 2007.
21. Locke BR, Shih KY. Review of the methods to form hydrogen peroxide in electrical discharge plasma with liquid water. *Plasma Sources Sci Technol*. 2011;20:034006.
22. Oehmigen K, Hahnel M, Brandenburg R, Wilke Ch, Weltmann KD, Woedtke Th von. The role of acidification for antimicrobial activity of atmospheric pressure plasma in liquids. *Plasma Process Polym*. 2010;7:250–257.
23. Tang YZ, Lu XP, Laroussi M, Dobbs FC. Sublethal and killing effects of atmospheric-pressure, nonthermal plasma on eukaryotic microalgae in aqueous media, *Plasma Process Polym*. 2008;5:552–558.
24. Lerouge S, Wertheimer MR, Marchand R, Tabrizian M, Yahia LH. Effect of gas composition on spore mortality and etching during low-pressure plasma sterilization. *J Biomed Mater Res*. 2000;51:128–135.
25. Moisan M, Barbeau J, Moreau S, Pelletier J, Tabrizian M, Yahia LH. Low-temperature sterilization using gas plasmas: a review of the experiments and an analysis of the inactivation mechanisms. *Int J Pharm*. 2001;226:1–21.
26. Rossi F, Kylian O, Rauscher H, Hasiwa M, Gilliland D. Low pressure plasma discharges for the sterilization and decontamination of surfaces. *New J Phys*. 2009;11:115017

Manuscript received Mar. 10, 2012, revision received July 25, 2012, and final revision received Sept. 20, 2012.